**Severe steatosis and mild colitis are important for the early occurrence of hepatocellular carcinoma**

Takeki Sato, Atsunori Tsuchiya, Takashi Owaki, Masaru Kumagai, Satoko Motegi, Takahiro Iwasawa, Shunsuke Nojiri, Masahiro Ogawa, Suguru Takeuchi, Yusuke Watanabe, Yuzo Kawata, Hiroteru Kamimura and Shuji Terai

Division of Gastroenterology and Hepatology, Graduate School of Medical and Dental Sciences, Niigata University, 1-757, Asahimachi-dori, Chuo-ku, Niigata, 951-8510, Japan.

**Corresponding authors:** Atsunori Tsuchiya and Shuji Terai
Address: Niigata University, 1-757 Asahimachi-dori, Chuo-ku, Niigata, 951-8510, Japan
Tel.: +81-25-227-2207
Fax: +81-25-227-0776
E-mail address: atsunori@med.niigata-u.ac.jp (A.T.), terais@med.niigata-u.ac.jp (S.T.)

**Footnote:** NASH, non-alcoholic steatohepatitis; IBD, inflammatory bowel disease; HCC, hepatocellular carcinoma; MC4R, melanocortin-4 receptor; HFD, high-fat diet; DSS, dextran sulfate sodium; ALB, albumin ; ALT, aminotransferase ; NAFLD, non-alcoholic fatty liver disease; PAMPs, pathogen-associated molecular patterns; LPS, lipopolysaccharide; CD, Crohn disease; UC, ulcerative colitis; SC, standard chow; WD, Western diet; DAI, Disease Activity Index; H&E, hematoxylin and eosin; AST, aspartate

transaminase; Bil, total bilirubin; NAS, NAFLD activity score; TLRs, toll like receptors; CDHF, choline-deficient high fat

**Abstract**

The number of patients with non-alcoholic steatohepatitis (NASH) and inflammatory bowel disease (IBD) is increasing. This study elucidates the effect of both NASH and IBD on hepatocellular carcinoma (HCC) using a mouse model combining NASH and IBD. The melanocortin 4 receptor-deficient (*Mc4r*-KO) mice were divided into four groups with or without a high-fat diet (HFD) and with or without dextran sulfate sodium (DSS) to induce colitis, and the differences in liver damage and occurrence of HCC were analyzed. In the HFD+DSS group, the body weight, liver weight/body weight ratio, and serum levels of albumin and alanine aminotransferase were significantly lower than those in the HFD group. We further found that steatosis was significantly lower and lobular inflammation was significantly higher in the HFD+DSS group than those in the HFD group, and that individual steatosis and lobular inflammation state in the HFD+DSS mice varied. We detected HCC only in the HFD+DSS group, and mice with severe steatosis and mild colitis were found to be at high risk of HCC. Presently, the prediction of HCC is very difficult. In some cases, severe colitis reverses the fat accumulation due to appetite loss. Our findings clearly showed that severe steatohepatitis and mild colitis are simultaneously essential for the occurrence of HCC in patients with NASH and IBD.

**Keywords:** Dextran sulfate sodium, Hepatocellular carcinoma, Inflammatory bowel disease, Melanocortin-4 receptor, Non-alcoholic steatohepatitis

## 1. Introduction

Patients with non-alcoholic fatty liver disease (NAFLD) comprise about 20% to 30% of the global population [1, 2]. NAFLD is one of the phenotypes of metabolic syndrome and is related to several factors such as insulin resistance, hyperlipidemia, and hypertension. About 20% to 30% of these patients develop nonalcoholic steatohepatitis (NASH) comprising inflammation with subsequent accumulation of fibrosis and ultimately progression to cirrhosis and/or hepatocellular carcinoma (HCC) [3, 4]. The multiple parallel hit hypothesis states that exposure to several factors, such as oxidative stress and gut-derived endotoxins, induce the transition of the simple fatty liver from NAFLD to NASH, cirrhosis, and HCC [5, 6]. Although it has been recognized that patients with NASH are at high risk of HCC and the exceptionally high incidence of NASH, these patients are not often evaluated and followed up with regularly.

One of the factors that affect the development of NASH comprises the substances from the intestinal tract. Intestinal flora or some parts of them called pathogen-associated molecular patterns (PAMPs) are well-known to cause inflammation followed by fibrosis formation [6, 7]. Bessissow et al. reported that activity of IBD and duration with IBD can affect the cause of NAFLD [8]. Indeed, to form the NASH model mouse, lipopolysaccharide (LPS) is often employed and an increase of liver damage and

progression of fibrosis is often confirmed [9]. On the other hand, recently the number of patients with inflammatory bowel disease (IBD) that include Crohn's disease (CD) and ulcerative colitis (UC) are increasing, implying that HCC can arise from patients with NASH and IBD [8, 10-12]. However, in patients with NASH and IBD, the disease state affecting the occurrence of HCC is not well-known.

Melanocortin 4 receptor-deficient (*Mc4r*-KO) mice and dextran sulfate sodium (DSS)-induced colitis models are representative NASH and IBD mice models, respectively. MC4R is expressed in the hypothalamic nuclei, where it regulates food intake and body weight; hence, *Mc4r*-KO mice cannot control their appetite and exhibit symptoms similar to those in human NASH, such as obesity, insulin resistance, and liver steatosis. When high-fat diet (HFD) was started 8 weeks after birth, steatohepatitis with fibrosis was observed 28 weeks after birth, and HCC occurred approximately 1 y after birth [13, 14]. Thus, the effect of drugs used for treating steatosis, fibrosis, and carcinogenesis can be evaluated using this mouse model. Oral intake of DSS can induce mainly colitis, and bloody stool, diarrhea, and body weight loss is observed in this model; depending on the severity of colitis, the colon length becomes short [15]. This study aimed to elucidate the effect of both NASH and IBD disease states on the occurrence of HCC, by combining and analyzing the representative NASH and IBD mouse models.

## 2. Methods

### 2.1. Mice

The male *Mc4r*-KO mice with a C57BL/6J background were provided by Joel K. Elmquist (University of Texas Southern Medical Center, Dallas, TX, USA). The animals were housed in a specific pathogen-free environment and kept under standard conditions with a 12-h day/night cycle and access to food and water ad libitum. All the animal experiments were conducted in compliance with the regulations and approval of the Institutional Animal Care Committee of the Niigata University.

### 2.2. Induction of experimental colitis

To induce colitis 1.0% DSS (molecular weight 36,000–50,000; MP Biomedicals, Irvine, CA, USA) was administered via drinking water. The colitis was induced repeatedly for 6 cycles. Each cycle consisted of 7 days of DSS administration followed by ceasing DSS for 14 days during which normal water was administrated.

### 2.3. Study design

All the mice used were fed a standard chow (SC; CE-2; CLEA Japan, Inc. Tokyo, Japan) until 8 weeks. The study started at 8 weeks and was conducted using only male

mice. The NASH model mice were developed using Western diet (WD; Research Diets, Inc., New Brunswick, NJ, USA)-fed-*Mc4r*-KO mice from 8 weeks of age. The mice were divided into the following groups: group 1, the mice administered SC for 26 weeks orally (SC group); group 2, the mice orally administered SC and low-dose DSS treatment (repeat of one-week oral intake of DSS and two weeks rest) from 8 weeks until 26 weeks (SC+DSS group); group 3, the mice administered HFD from 8 weeks until 26 weeks (HFD group); and group 4, group 3 mice that were administered low-dose DSS treatment from 8 weeks until 26 weeks (HFD+DSS group). In group 4, liver carcinogenesis was observed in some mice. Therefore, group 4 was further divided into HDF+DSS non-cancer group and HFD+DSS cancer group for further analysis (Supplemental Figure 1). Twenty-six weeks after birth, all the mice were sacrificed and analyzed.

**2.4. Evaluation of the colon**

To evaluate the colon, the disease activity index (DAI), the colon length, and histological score were analyzed. DAI was calculated by the combined scores of weight loss, stool consistency, and bleeding divided by 3, as described previously [15]. The colon lengths were measured from the anus to the cecum soon after harvesting the

colon. The histological score was calculated as follows. The colon was excised, fixed in 10% formalin, embedded in paraffin wax, and sliced into 4-μm-thick sections. After hematoxylin and eosin (H&E) staining, histological evaluation was performed in a blinded fashion according to a previously published scoring system [16]. Briefly, the total colitis score was the sum of the three sub-scores (inflammation severity 0–3 points, inflammation extent 0–3 points, and crypt damage 0–4 points), which were multiplied by the degree of inflammation involvement as follows: × 1: 1%–25%; × 2: 26%–50%; × 3: 51%–75%; × 4: 76%–100%. The distal colon was used in the experiment because the inflammation of the distal colon was severe and the inflammation of the proximal colon was mild.

**2.5. Serum analyses**

Blood samples were obtained from the hearts of mice at 18 weeks after the start of the experiment. Serum alanine aminotransferase (ALT), aspartate transaminase (AST), total bilirubin (Bil), and albumin (ALB) concentrations were determined by Oriental Yeast Co., Ltd., Nagahama LSL (Nagahama, Japan).

**2.6. Evaluation of the liver and immunohistochemistry**

For immunohistochemistry, the tissues were fixed in 10% formalin and cut into 4-μm-thick sections. The paraffin sections were deparaffinized, rehydrated, and stained with H&E and Sirius Red for histological examination following the manufacturer's standard protocols.

Immunohistochemistry for F4/80 (Abcam, Cambridge, UK; ab111101; rabbit monoclonal to F4/80, dilution 1/100) was performed as follows. Where necessary, sections were subjected to antigen retrieval by heating the sample in the appropriate buffer (10 mM sodium citrate buffer at pH 6.0 or 1 mM EDTA buffer at pH 8.0). The endogenous peroxidase activity was blocked by treatment with 3% $H_2O_2$ in PBS for 10 min at 20–25 ℃, followed by avidin-biotin blocking. The samples were incubated with the primary antibody overnight at 4 °C. Subsequently, the species-specific biotinylated anti-IgG antibodies were used for detection. Slides were then stained using the Vectastain® ABC kit (Vector Laboratories, Inc. Burlingame, CA, USA) and the DAB substrate (Muto Pure Chemicals, Tokyo, Japan). The nuclei were stained using the hematoxylin solution (Vector Laboratories, Inc.).

NASH was evaluated based on the NAFLD activity score (NAS) using steatosis (0–3), lobular inflammation (0–3), and ballooning hepatocellular swelling (0–2). Samples with NAS ≥ 5 were diagnosed as NASH [17].

The photographs were captured for each section randomly (3 fields/mouse) using a BZ-9000 microscope (Keyence, Osaka, Japan), and quantitative analysis of the fibrotic area was performed using the ImageJ software (version 1.6.0 20, National Institutes of Health, Bethesda, MD, USA).

### 2.7. Hydroxyproline assay

The levels of hydroxyproline, a representative collagen component, were determined at 18 weeks after the start of the experiment. The liver samples (20 mg) were homogenized and subjected to QuickZyme Hydroxyproline Assays (QuickZyme Bioscience, Zernikedreef, the Netherlands) according to the manufacturer's protocol. The samples were extracted, and absorbance was measured at 570 nm. Data were expressed as the amount of hydroxyproline per mg liver tissue.

### 2.8. Statistical analyses

Statistical analyses were performed by using the GraphPad Prism8 software (GraphPad Software Inc., La Jolla, CA, USA) and Microsoft Excel (Microsoft, Washington, DC, USA). Data are represented as means ± standard error of the mean. Differences between groups were analyzed by the Kruskal–Wallis test followed by Dunn's Test. Differences

with *p* values less than 0.05 were considered significant. The 3-axis graph was created using the XLSTAT software (Addinsoft Inc, New York, NY, USA).

## 3. Results

### 3.1. Establishment of NASH with colitis model to evaluate the occurrence of HCC

To evaluate whether colitis increase the occurrence of HCC in NASH, we divided the *Mc4r*-KO mice into four groups based on diet and DSS treatment. Body weight in the HFD groups (group 3 and 4) was higher than that in SC groups (group 1 and 2). In addition, body weight in the DSS treated groups (group 2 and 4) was significantly lower than that in the corresponding control groups (group 1 and 3) (Figure 1A). We focused our analysis on the comparison between HFD and HFD+DSS groups. Body weight (HFD: 47.43 ± 0.44 g, HFD+DSS: 41.79 ± 0.78 g, $p < 0.01$), liver weight/body weight ratio (HFD: 9.06 ± 0.20%, HFD+DSS: 6.75 ± 0.19%, $p < 0.01$) (Figure 1B, C), as well as serum levels of ALB (HFD: 3.42 ± 0.04 g/dL, HFD+DSS: 2.78 ± 0.04 g/dL, $p < 0.01$; Figure 1D) and ALT (HFD: 348.73 ± 26.51 IU/L, HFD+DSS: 183.15 ± 15.89 IU/L, $p < 0.01$) were significantly lower in the HFD+DSS group than those in the HFD group (Figure 1E-G). We further evaluated steatosis, lobular inflammation, ballooning based on NAS. While ballooning was not significantly different between the HFD and HFD+DSS groups (HFD: 2.00± 0.00, HFD+DSS: 1.84 ± 0.04, $p = 0.74$), steatosis

(HFD: 3.00 ± 0.00, HFD+DSS: 2.10 ± 0.09, $p < 0.01$) in HFD+DSS group was significantly lower than that in HFD group and lobular inflammation (HFD: 0.18 ± 0.06, HFD+DSS: 0.73 ± 0.08, $p < 0.01$) in HFD+DSS group was significantly higher than that in HFD group. Although total NAS was not significantly different between the two groups (HFD: 5.18 ± 0.06, HFD+DSS: 4.67 ± 0.17, $p > 0.99$), we found that individual steatosis and lobular inflammation state in the HFD+DSS mice were different (Figure 1H–K).

### 3.2. Colon pathological score inversely correlated with the colon length

Next, we calculated DAI score, which evaluates weight loss, stool consistency, bleeding, in the SC+DSS and HFD+DSS groups. Both groups showed similar dynamics; the DAI score increased during DSS treatment and decreased after stopping the DSS treatment. These cycles were repeated 6 times, and the maximum DAI score increased approximately up to 2 (Figure 2A). The colon length in the SC and HFD groups was significantly longer than in the corresponding groups (SC: 101.75 ± 3.35 cm, SC+DSS: 80.72 ± 1.98 cm, $p < 0.01$; HFD: 98.20 ± 0.89 cm, HFD+DSS: 79.86 ± 1.06 cm, $p < 0.01$; Figure 2B). We further observed that the colon pathological score inversely correlated with the colon length in both DSS-treated groups (SC+DSS: r=-

0.8562, HFD+DSS r=-0.6598; Figure 2C, D).

### 3.3. Liver tumors were detected only in the HFD+DSS group

To evaluate the liver damage in the four groups, liver fibrosis was evaluated by Sirius Red staining and quantitative hydroxyproline, and the number of F4/80+ macrophages were counted. A marked difference was observed between the HFD and the HFD+DSS groups with respect to fibrosis. While there were individual differences in fibrosis in the HFD+DSS group, both Sirius Red staining area (HFD: 1.08 ± 0.12%, HFD+DSS: 3.27 ± 0.24%, $p < 0.01$) and quantitative hydroxyproline (HFD: 2.17 ± 0.15 nmol/mg, HFD+DSS: 2.70 ± 0.12 nmol/mg, $p = 0.03$) were significantly higher in the HFD+DSS group than HFD group (Figure 3A–C). In both the SC+DSS and HFD+DSS groups, the number of macrophages was greater than that in the corresponding non-treated groups (SC: 0.27± 0.05%, SC+DSS: 2.59 ± 0.17%, $p < 0.01$; HFD: 1.67 ± 0.08%, HFD+DSS: 3.17 ± 0.16%, $p < 0.01$; Figure 3D, E). Moreover, we found that the HCC could be detected only in the HFD+DSS group (5/82 mice, 6.1%) (Figure 3F, G).

### 3.4. Severe steatosis and mild colitis are important for the occurrence of HCC

To analyze the characteristics of mice with HCC, we divided the HFD+DSS group into

an HFD+DSS non-cancer group and an HFD+DSS cancer group and compared them with the HFD group. The most notable difference between the HFD+DSS non-cancer group and the HFD+DSS cancer group was the degree of body weight gain. In the HFD+DSS cancer group, DSS administration did not change the body weight compared to the control group until approximately 70 days after birth; however, in the HFD+DSS non-cancer group, the body weight was lower compared to that of the HFD group, and HFD+DSS cancer group (Figure 4A–C). Next, we analyzed the serum data (Figure 4D–G), fibrosis (Figure 4H, I), number of macrophages (Figure 4J), colon length (Figure 4K), and NAS (steatosis, lobular inflammation, and ballooning; Figure 4L–N) in these groups. While a significant difference was not observed owing to the low number of animals in the HFD+DSS cancer groups, the HFD+DSS cancer group showed a tendency towards middle-length colon, severe steatosis, high number of macrophages, and fibrosis. We finally showed the distribution of the HFD+DSS cancer group by a three-dimensional orthogonal coordinate system using three parameters—colon length, NAS, and colon pathological score, and found that in the HFD+DSS cancer group, NAS high, colon length middle, and low colon pathological score area were evident (Figure 4O).

## 4. Discussion

In this study, we elucidated that severe steatosis and mild colitis are important for the early occurrence of HCC using *Mc4r*-KO mice with DSS-induced colitis. HCC can occur in *Mc4r*-KO mice with HFD approximately one year after birth; however, in the HFD+DSS model, progression of fibrosis and HCC was detected only 26 weeks after birth. Our results clearly showed that mild but not severe inflammation of the colon is a very important factor for the occurrence of HCC.

Four papers mentioned the different aspects of the IBD and NAFLD. Principi et al. reported that NAFLD is more common and occurred at a younger age in IBD subjects than in non-IBD subjects [12]. Sourianaryanane et al. reported that among 928 IBD patients, 76 (8.2%) had NAFLD, and patients not receiving anti-tumor necrosis factor-alpha (TNF-α) therapy had a higher occurrence of NAFLD. They also reported that hypertension, obesity, small bowel surgeries, and the use of steroids were independent factors associated with NAFLD [10]. Bessissow et al. performed a retrospective study of 321 IBD patients without liver disease and followed a median of 3.2 years for the occurrence of NAFLD. They found that 108 (33.6%) patients developed NAFLD and 7 (2.2%) patients developed advanced liver fibrosis. Thus, they concluded that NAFLD

results in frequent comorbidity in patients with IBD and disease activity, duration of IBD, and prior surgery is a predictor of NAFLD development [8]. On the other hand, Sartini et al. compared the clinical and metabolic features of NAFLD in 223 patients with (n = 78) and without IBD (n = 145). They found that more than one IBD relapse per year during the disease course and more extensive intestinal involvement were independent risk factors of NAFLD. They also found that the ongoing anti-TNF-α therapy was the only independent factor that prevents alteration of the liver enzymes [11]. These four studies mentioned the relationship between the IBD and NAFLD; however, they do not mention the occurrence of HCC. Long-term study to follow the occurrence of HCC in patients with IBD and NAFLD will be necessary in the future. In our study, severe colitis did not necessarily induce severe hepatitis. The studies in humans were different from those in mice in this respect. In mice, severe colitis was suspected to lead to appetite loss even in the *Mc4r*-KO mice who could not control their appetite. Therefore, steatosis was improved in mice with severe colitis. In humans, on the contrary, long-term severe IBD was found to cause severe malnutrition, inducing steatosis. Although the situation is mildly different between humans and mice, steatosis with colitis can hence be a risk factor for the occurrence of HCC.

The gut microbiome is well known as one of the most important components of the

multiple parallel hit hypothesis. Rahman et al. reported that NAFLD conditions induced by a HFD (among other factors) result in the loss of a junctional molecule and induce severe steatohepatitis [18]. This can cause the translocation of intestinal bacteria and/or bacterial components termed PAMPs. These bacteria and PAMPs can cause inflammation through toll-like receptors (TLRs). It is well known that PAMPs from intestinal microbiota and TLR-4 contribute to the development of liver fibrosis [3, 19, 20]. Intestinal inflammation is another important factor for bacterial and PAMP translocation. Intestinal inflammation can cause damage to the intestinal barrier and gut–vascular barrier dysfunction. In addition, intestinal inflammation can induce dysbiosis [7, 21]. All these phenomena can increase the bacterial and PAMP translocation and may lead to hepatitis followed by fibrosis. Dapito et al. further reported that TLR4 and the intestinal microbiota were not required for HCC initiation but HCC promotion, mediating increased proliferation, expression of hepatomitogen epiregulin, and prevention of apoptosis [22]. Similarly, Achiwa et al. reported that mice with DSS-induced colitis fed a choline-deficient high fat (CDHF) diet might have a high frequency of HCC (4/11, 36.4%) in 12 weeks [23]. However, the difference between their study and our study lies in the NASH mice model. Our model can induce obesity and insulin resistance similar to that in humans, whereas the CDHF diet-fed mice did

not gain or lose weight during the experiment. Our animal model would be important to evaluate the pathology of steatohepatitis, fibrosis, and HCC.

The limitation of this study is that we could not find the difference in the substances from the intestine, such as specific PAMPs. Future study is necessary to detect these substances or strengthen the gut–vascular barrier to expand our knowledge for prevention of steatohepatitis, fibrosis, and HCC. However, our study provides an appropriate model of HCC with NASH and IBD to study the development of HCC.

**Financial support**

This research was supported by a Grant-in-Aid for Scientific Research (C) (18K07903) from the Ministry of Education, Culture, Sports, Science and Technology of Japan.

**Acknowledgments**

We thank Takao Tsuchida for his cooperation in the preparation of pathological tissue.

**Disclosures**

The authors declare no conflict of interest.

## Author contributions

TS and AT proposed the study and drafted the manuscript. TS, AT, TO, MK, SM, TI, SN, MO, SGT, YW, YK and HK performed the experiments. SH-T provided critical comments and edits to the manuscript. All authors approved the final version of the manuscript.

## References

[1] G. Vernon, A. Baranova, Z.M. Younossi, Systematic review: the epidemiology and natural history of non-alcoholic fatty liver disease and non-alcoholic steatohepatitis in adults, Aliment Pharmacol Ther, 34 (2011) 274-285.

[2] Z.M. Younossi, A.B. Koenig, D. Abdelatif, Y. Fazel, L. Henry, M. Wymer, Global epidemiology of nonalcoholic fatty liver disease-Meta-analytic assessment of prevalence, incidence, and outcomes, Hepatology, 64 (2016) 73-84.

[3] G.C. Farrell, C.Z. Larter, Nonalcoholic fatty liver disease: from steatosis to cirrhosis, Hepatology, 43 (2006) S99-S112.

[4] C.D. Williams, J. Stengel, M.I. Asike, D.M. Torres, J. Shaw, M. Contreras, C.L. Landt, S.A. Harrison, Prevalence of nonalcoholic fatty liver disease and nonalcoholic steatohepatitis among a largely middle-aged population utilizing ultrasound and liver biopsy: a prospective study, Gastroenterology, 140 (2011) 124-131.

[5] H. Tilg, A.R. Moschen, Evolution of inflammation in nonalcoholic fatty liver disease: the multiple parallel hits hypothesis, Hepatology, 52 (2010) 1836-1846.

[6] E. Gabele, K. Dostert, C. Hofmann, R. Wiest, J. Scholmerich, C. Hellerbrand, F. Obermeier, DSS induced colitis increases portal LPS levels and enhances hepatic inflammation and fibrogenesis in experimental NASH, J Hepatol, 55 (2011) 1391-1399.

[7] C. Cheng, J. Tan, W. Qian, L. Zhang, X. Hou, Gut inflammation exacerbates hepatic injury in

the high-fat diet induced NAFLD mouse: Attention to the gut-vascular barrier dysfunction, Life Sci, 209 (2018) 157-166.
[8] T. Bessissow, N.H. Le, K. Rollet, W. Afif, A. Bitton, G. Sebastiani, Incidence and Predictors of Nonalcoholic Fatty Liver Disease by Serum Biomarkers in Patients with Inflammatory Bowel Disease, Inflamm Bowel Dis, 22 (2016) 1937-1944.
[9] T. Watanabe, A. Tsuchiya, S. Takeuchi, S. Nojiri, T. Yoshida, M. Ogawa, M. Itoh, M. Takamura, T. Suganami, Y. Ogawa, S. Terai, Development of a non-alcoholic steatohepatitis model with rapid accumulation of fibrosis, and its treatment using mesenchymal stem cells and their small extracellular vesicles, Regen Ther, 14 (2020) 252-261.
[10] A. Sourianarayanane, G. Garg, T.H. Smith, M.I. Butt, A.J. McCullough, B. Shen, Risk factors of non-alcoholic fatty liver disease in patients with inflammatory bowel disease, J Crohns Colitis, 7 (2013) e279-285.
[11] A. Sartini, S. Gitto, M. Bianchini, M.C. Verga, M. Di Girolamo, A. Bertani, M. Del Buono, F. Schepis, B. Lei, N. De Maria, E. Villa, Non-alcoholic fatty liver disease phenotypes in patients with inflammatory bowel disease, Cell Death Dis, 9 (2018) 87.
[12] M. Principi, A. Iannone, G. Losurdo, M. Mangia, E. Shahini, F. Albano, S.F. Rizzi, R.F. La Fortezza, R. Lovero, A. Contaldo, M. Barone, G. Leandro, E. Ierardi, A. Di Leo, Nonalcoholic Fatty Liver Disease in Inflammatory Bowel Disease: Prevalence and Risk Factors, Inflamm Bowel Dis, 24 (2018) 1589-1596.
[13] M. Itoh, T. Suganami, N. Nakagawa, M. Tanaka, Y. Yamamoto, Y. Kamei, S. Terai, I. Sakaida, Y. Ogawa, Melanocortin 4 receptor-deficient mice as a novel mouse model of nonalcoholic steatohepatitis, Am J Pathol, 179 (2011) 2454-2463.
[14] T. Yoshida, A. Tsuchiya, M. Kumagai, S. Takeuchi, S. Nojiri, T. Watanabe, M. Ogawa, M. Itoh, M. Takamura, T. Suganami, Y. Ogawa, S. Terai, Blocking sphingosine 1-phosphate receptor 2 accelerates hepatocellular carcinoma progression in a mouse model of NASH, Biochem Biophys Res Commun, 530 (2020) 665-672.
[15] H.S. Cooper, S.N.S. Murthy, R.S. Shah, D.J. Sedergran, Clinicopathological Study of Dextran Sulfate Sodium Experimental Murine Colitis, Lab Invest, 69 (1993) 238-249.
[16] K.L. Williams, C.R. Fuller, L.A. Dieleman, C.M. DaCosta, K.M. Haldeman, R.B. Sartor, P.K. Lund, Enhanced survival and mucosal repair after dextran sodium sulfate-induced colitis in transgenic mice that overexpress growth hormone, Gastroenterology, 120 (2001) 925-937.
[17] D.E. Kleiner, E.M. Brunt, M. Van Natta, C. Behling, M.J. Contos, O.W. Cummings, L.D. Ferrell, Y.C. Liu, M.S. Torbenson, A. Unalp-Arida, M. Yeh, A.J. McCullough, A.J. Sanyal, N. Nonalcoholic Steatohepatitis Clinical Research, Design and validation of a histological scoring system for nonalcoholic fatty liver disease, Hepatology, 41 (2005) 1313-1321.
[18] K. Rahman, C. Desai, S.S. Iyer, N.E. Thorn, P. Kumar, Y. Liu, T. Smith, A.S. Neish, H. Li,

S. Tan, P. Wu, X. Liu, Y. Yu, A.B. Farris, A. Nusrat, C.A. Parkos, F.A. Anania, Loss of Junctional Adhesion Molecule A Promotes Severe Steatohepatitis in Mice on a Diet High in Saturated Fat, Fructose, and Cholesterol, Gastroenterology, 151 (2016) 733-746 e712.
[19] A. Spruss, G. Kanuri, S. Wagnerberger, S. Haub, S.C. Bischoff, I. Bergheim, Toll-like receptor 4 is involved in the development of fructose-induced hepatic steatosis in mice, Hepatology, 50 (2009) 1094-1104.
[20] C.A. Rivera, P. Adegboyega, N. van Rooijen, A. Tagalicud, M. Allman, M. Wallace, Toll-like receptor-4 signaling and Kupffer cells play pivotal roles in the pathogenesis of non-alcoholic steatohepatitis, J Hepatol, 47 (2007) 571-579.
[21] K. Brandl, B. Schnabl, Is intestinal inflammation linking dysbiosis to gut barrier dysfunction during liver disease?, Expert Rev Gastroenterol Hepatol, 9 (2015) 1069-1076.
[22] D.H. Dapito, A. Mencin, G.Y. Gwak, J.P. Pradere, M.K. Jang, I. Mederacke, J.M. Caviglia, H. Khiabanian, A. Adeyemi, R. Bataller, J.H. Lefkowitch, M. Bower, R. Friedman, R.B. Sartor, R. Rabadan, R.F. Schwabe, Promotion of hepatocellular carcinoma by the intestinal microbiota and TLR4, Cancer Cell, 21 (2012) 504-516.
[23] K. Achiwa, M. Ishigami, Y. Ishizu, T. Kuzuya, T. Honda, K. Hayashi, Y. Hirooka, Y. Katano, H. Goto, DSS colitis promotes tumorigenesis and fibrogenesis in a choline-deficient high-fat diet-induced NASH mouse model, Biochem Biophys Res Commun, 470 (2016) 15-21.

## Figure Legends

**Figure 1. Analysis of changes in body weight, serum data, and NAS.** Body weight changes (A), body weight (B), and liver weight/body weight ratio (C) 26 weeks after birth. Serum levels of ALB (D), AST (E), ALT (F), and T-Bil (G). NAS (H) and its parameters, namely steatosis (I), lobular inflammation (J), ballooning (K) in all groups. SC, standard chow; HFD, high-fat diet; DSS, dextran sulfate sodium. SC group (n=8), SC+DSS group (n = 25), HFD group (n = 40), HFD+DSS (n = 82). Data are presented as mean ± standard error of the mean. *$p < 0.05$, **$p < 0.01$.

**Figure 2. DAI score, colon length, and pathological score**. Serial daily DAI score of the SC+DSS group and HFD+DSS group (A). Colon length 26 weeks after birth (B). HE staining of each group. Scale bar, 100 μm (C). The relationship between colon length and colon pathological score (D). SC, standard chow; HFD, high-fat diet; DSS, dextran sulfate sodium; H&E, hematoxylin and eosin. Data are presented as means ± standard error of the mean. $^{**}p < 0.01$.

**Figure 3. Evaluation of fibrosis, macrophages, and HCC occurrence.** Sirius red staining (A), positive area of Sirius red staining (B), and quantitative of hydroxyproline (C). Immunohistochemistry of F4/80 (D) and its staining area (E). H&E staining of liver and HCC in the liver and macroscopic image of HCC (F). Tumor incidence in each group (G). The bars indicate the means of each data set. White arrow heads indicate the hepatocellular carcinomas. Scale bar, 100 μm. H&E; hematoxylin and eosin. $^{*}p < 0.05$, $^{**}p < 0.01$.

**Figure 4. Analysis of the occurrence of HCC in HFD+DSS group.** Serial body weight changes in the HFD, HFD+DSS non-cancer, and HFD+DSS cancer groups. Data are presented as means ± standard error of the mean. (A). Bodyweight (B) and liver weight/body weight ratio (C) 26 weeks after birth. Serum levels of ALB (D), AST (E), ALT (F), and T-Bil (G). Positive area of Sirius red staining (H), and quantitative of

hydroxyproline (I). F4/80 staining area (J) and colon length (K). Steatosis (L), lobular inflammation (M), ballooning (N) (data are presented as means ± standard error of the mean). A three-dimensional image showing the relationship between NAS, colon length, and colon pathological score (O). The bars indicate the means of each data set. *$p < 0.05$, **$p < 0.01$.

**Supplemental Figure 1. Scheme of this study.**

Figure 1

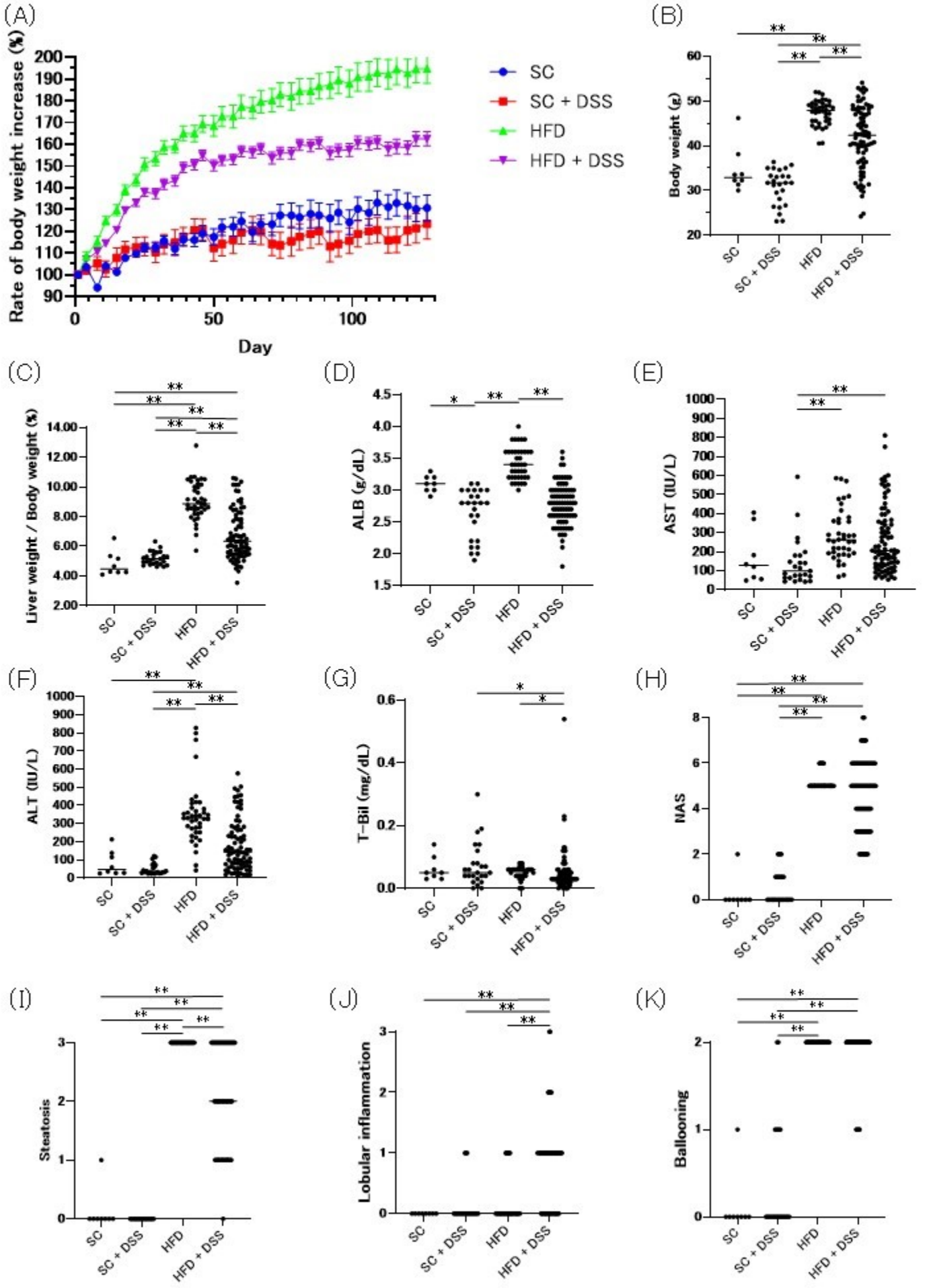
(A)
Rate of body weight increase (%)
Day
SC
SC + DSS
HFD
HFD + DSS
(B)
Body weight (g)
(C)
Liver weight / Body weight (%)
(D)
ALB (g/dL)
(E)
AST (IU/L)
(F)
ALT (IU/L)
(G)
T-Bil (mg/dL)
(H)
NAS
(I)
Steatosis
(J)
Lobular inflammation
(K)
Ballooning

Figure 2

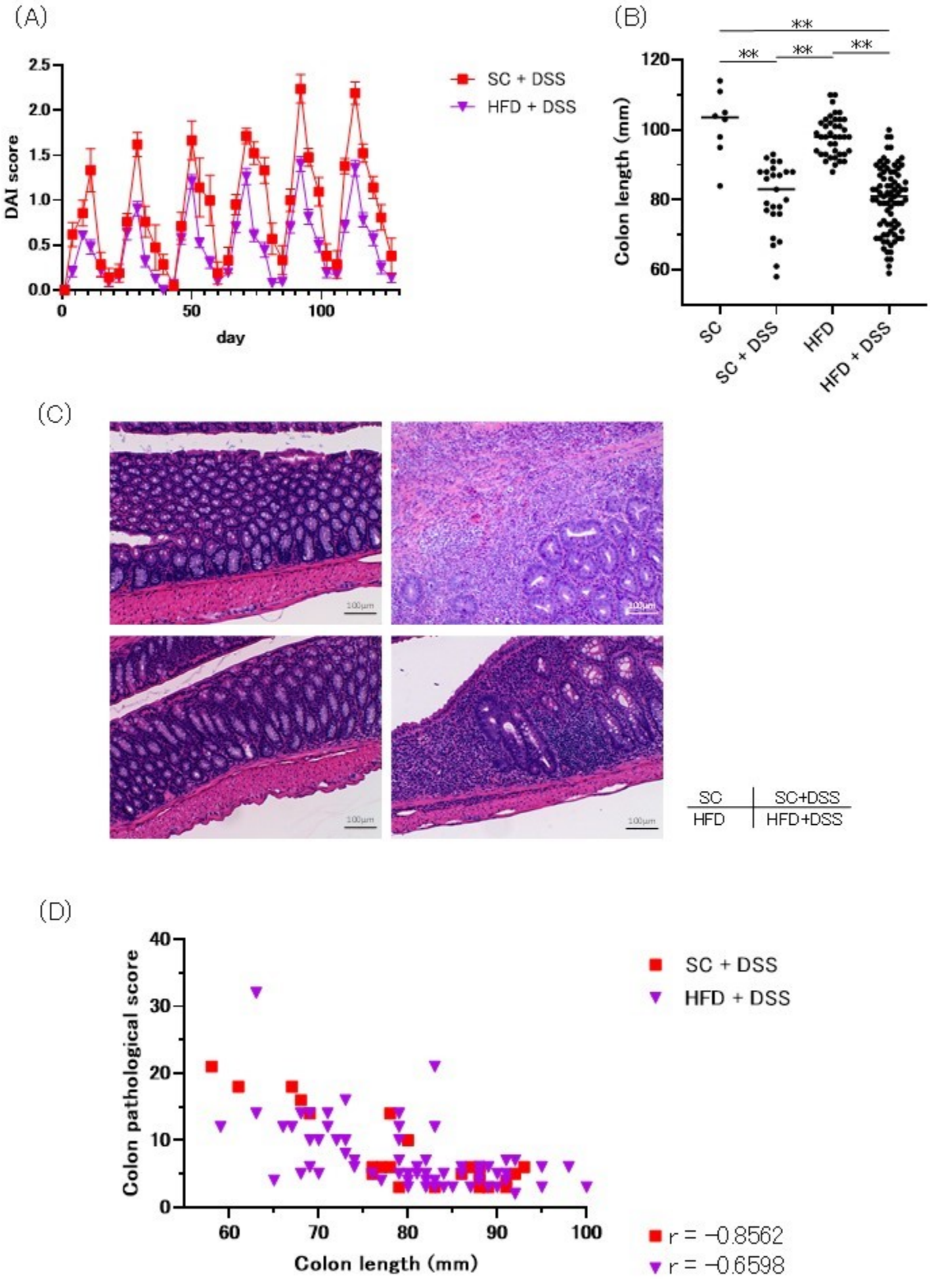
(A)
DAI score
day
SC + DSS
HFD + DSS
(B)
Colon length (mm)
SC
SC + DSS
HFD
HFD + DSS
**
(C)
SC
SC+DSS
HFD
HFD+DSS
(D)
Colon pathological score
Colon length (mm)
SC + DSS
HFD + DSS
r = −0.8562
r = −0.6598

Figure 3

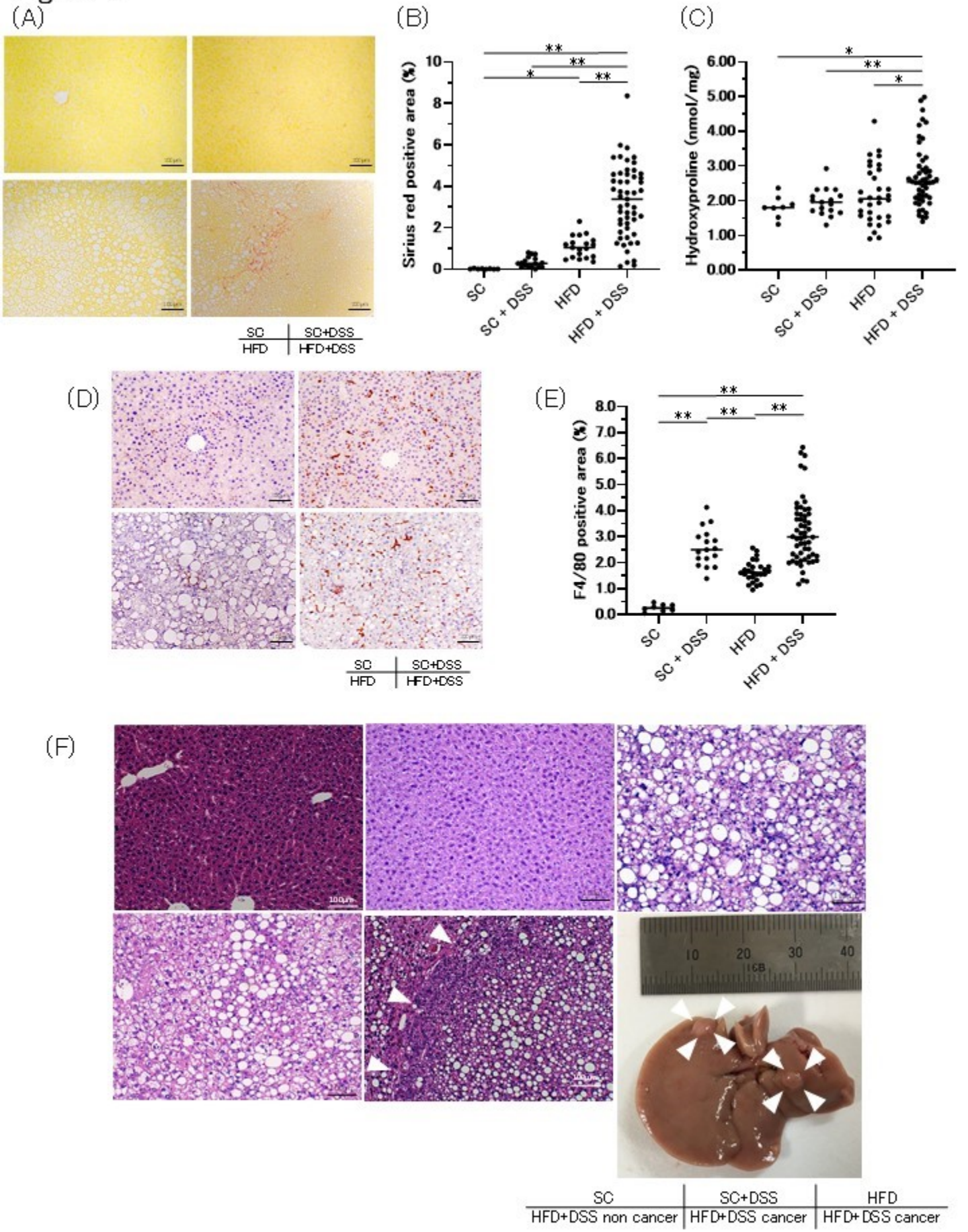


(G)

| diet | | SC | | HFD | |
|---|---|---|---|---|---|
| DSS | | − | + | − | + |
| cancer | + | 0 | 0 | 0 | 5 |
| | − | 8 | 25 | 40 | 77 |

Figure 4

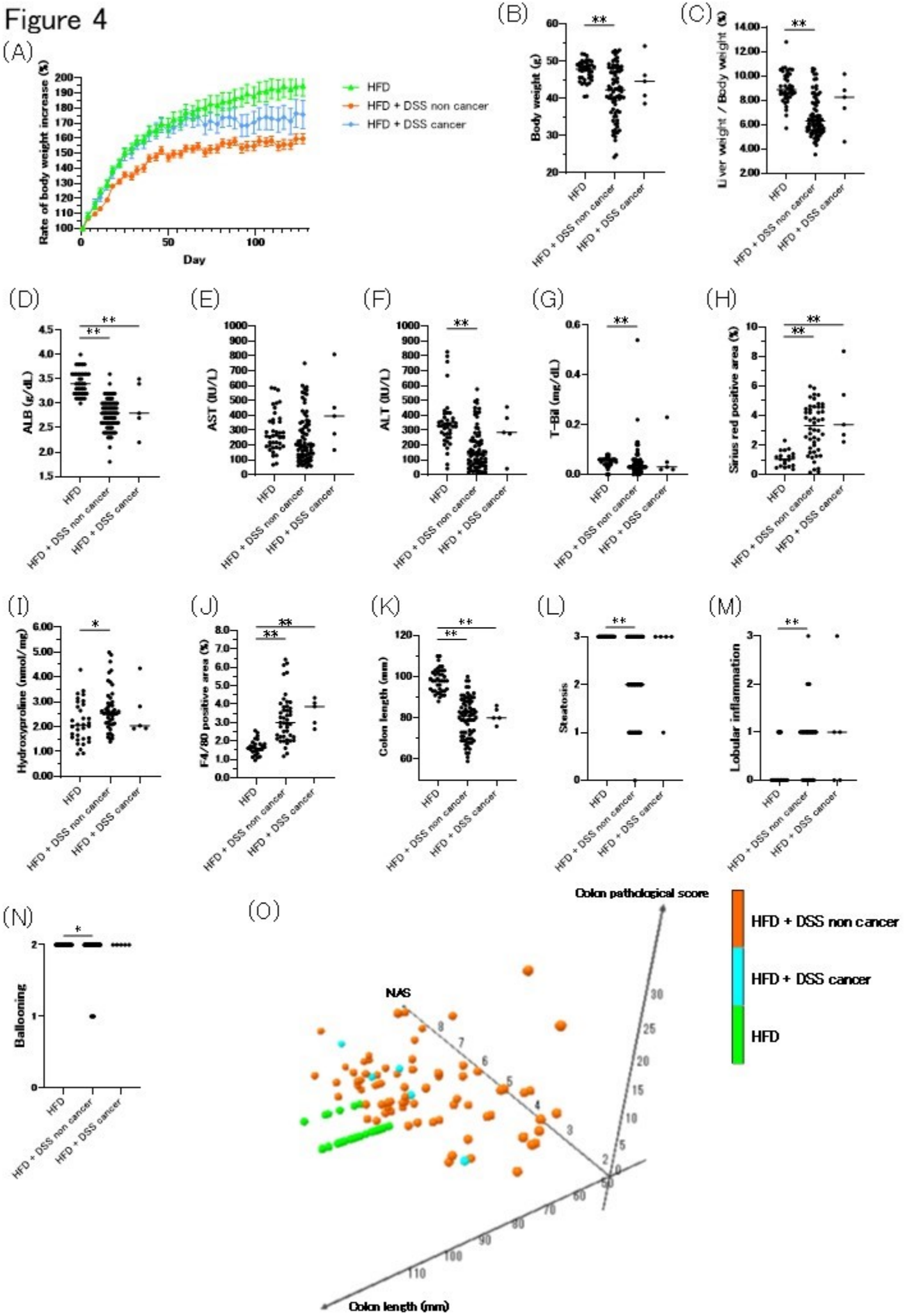
(A)
Rate of body weight increase (%)
Day
HFD
HFD + DSS non cancer
HFD + DSS cancer
(B)
Body weight (g)
(C)
Liver weight / Body weight (%)
(D)
ALB (g/dL)
(E)
AST (IU/L)
(F)
ALT (IU/L)
(G)
T-Bil (mg/dL)
(H)
Sirius red positive area (%)
(I)
Hydroxyproline (nmol/mg)
(J)
F4/80 positive area (%)
(K)
Colon length (mm)
(L)
Steatosis
(M)
Lobular inflammation
(N)
Ballooning
(O)
Colon pathological score
NAS
Colon length (mm)
HFD + DSS non cancer
HFD + DSS cancer
HFD

Supplemental Figure 1